JOURNAL OF DEGRADED AND MINING LANDS MANAGEMENT
Volume 10, Number 2 (January 2023):4073-4080, doi:10.15243/jdmlm.2023.102.4073
ISSN: 2339-076X (p); 2502-2458 (e), www.jdmlm.ub.ac.id

Research Article

The use of multi-sensor satellite imagery to analyze flood events and land cover changes using change detection and machine learning techniques in the Barito watershed

Muhammad Priyatna[1,2*], Sastra Kusuma Wijaya[2], Muhammad Rokhis Khomarudin[1], Fajar Yulianto[1], Gatot Nugroho[1], Pingkan Mayestika Afgatiani[1,3], Anisa Rarasati[1], Muhammad Arfin Hussein[4]

[1] Remote Sensing Research Center, Research Organization of Aeronautics and Space, The National Research and Innovation Agency (BRIN), Jakarta Timur, 13710, Indonesia
[2] Physics Department, Faculty of Mathematics and Natural Sciences, Universitas of Indonesia, Depok, 16424, Indonesia
[3] Faculty of Science, Graduate School of Science and Engineering, University of the Ryukyus, Okinawa, Japan
[4] Instrumentation Elctronics Studi Program, Politeknik Teknik Nuklir Indonesia, Jogyakarta, Indonesia

[*]corresponding author: muha054@brin.go.id

Article history:
Received 24 June 2022
Accepted 13 October 2022
Published 1 January 2023

Keywords:
Landsat-8
land use/land cover (LULC)
Otsu method
random forest
Sentinel-1

Abstract

Indonesia is one of the countries in the world that is frequently affected by floods. Flood disasters can have various negative impacts; therefore, they need to be analyzed to determine prevention and mitigation measures. This study examined land cover change, flood detection, and flood distribution using multitemporal Sentinel-1 and Landsat-8 satellite imagery in the Barito watershed. A combination of change detection and the application of the Otsu algorithm was used to detect floodplains from Sentinel-1 imagery. Land use/land cover (LULC) changes are detected using a combination of change detection and machine learning in the form of a random forest algorithm. The overlay technique was used to analyze the distribution of floodplains. In this study, the floodplain in the study area was mapped to 109,623 ha. The change detection method detects a decrease in the areas of primary forest, secondary forest, fields, rice fields, shrubs and ponds, respectively, by 13,020 ha, 116,235 ha, 259 ha, 146,696 ha, 47,308 ha, and 9,601 ha. Settlements, bare land, plantations and water bodies increase by 14,879 ha, 64,830 ha, 218,916 ha, and 34,768 ha, respectively. Flooding was mainly found in the classes of rice fields, water bodies and primary forests.

To cite this article: Priyatna, M., Wijaya, S.K., Khomarudin, M.R., Yulianto, F., Nugroho, G., Afgatiani, P.M., Rarasati, A. and Hussein, M.A. 2023. Use of multi-sensor satellite imagery to analyze flood events and land cover changes using change detection and machine learning techniques in the Barito watershed. Journal of Degraded and Mining Lands Management 10(2):4073-4080, doi:10.15243/jdmlm.2023.102.4073.

Introduction

Indonesia is one of the countries in the world that is frequently affected by floods (Rosyidie, 2013). Floods in Indonesia can occur in almost all parts of Indonesia. Floods can have several negative impacts, such as loss of housing (Echendu, 2020) and increased disease incidence (Ramakrishna et al., 2014). Flooding in agricultural areas can threaten food availability (Week and Wizor, 2020). Floodplain mapping is critical for planning future development activities. This mapping is beneficial for determining strategies to minimize the negative impacts caused by flooding (Echendu, 2020).

A variety of factors can cause flooding. Some factors can cause flooding (Savitri and Pramono, 2017). One of the causes of flooding is land use change

upstream and downstream (Sugianto et al., 2022). Changes in land use can affect watershed function (Maria and Lestiana, 2014). The watershed functions as a reservoir and storage for water in the watershed system (Anurogo, 2017). Watersheds as collectors are essential for controlling floods in watersheds (Wahyuni et al., 2017). The decline of watersheds means that the environment can no longer absorb the amount of stormwater that falls, resulting in flooding. Therefore, land use and land cover changes are needed to analyze flood events.

Remote sensing data have very great potential for flood analysis. Remote-sensing satellite images have excellent historical data (Lechner et al., 2020). Some satellite images, such as Lansat-8, Sentinel-1, and Sentinel-2, are even available and accessible to users free of charge (Traore et al., 2020; Nyamekye et al., 2021; Solórzano et al., 2021). These two advantages of data lead to the rapid development of remote sensing data use. Remote sensing data are also widely used to determine the location of floodplains. Radar satellite imagery from Sentinel-1 can detect flooding with reasonable accuracy (Amitrano et al., 2018; Uddin et al., 2019). Optical satellite imagery such as Landsat-8 and Sentinel-2 has proven to classify land use quite well (Nguyen et al., 2020; Talukdar et al., 2020).

Flooding can be detected with a single image after a flood event and with multitemporal images before and after a flood event (Shen et al., 2019; Huang and Jin, 2020). Land use changes are usually detected using multitemporal optical imagery (Yulianto et al., 2021). For tropical areas such as Indonesia, multitemporal imagery is necessary to minimize the influence of clouds on optical imagery (Yulianto et al., 2022). Previous studies have shown that puddles can be detected with optical imagery (Yulianto et al., 2022). Generally, the detection of standing water is performed using the Normalized Difference Water Index (NDWI) (Li et al., 2021). The NDWI is calculated using the normalized difference between the green band and the near-infrared optical image (Oezelkan, 2020). The separation of standing water and land is usually done using the threshold method for the NDWI value. The NDWI value that is commonly used as a threshold is zero (Acharya et al., 2017). However, the use of optical satellite imagery and NDWI for flood detection faces many obstacles because optical imagery is susceptible to weather interference (Amitrano et al., 2018).

Materials and Methods

Study area

This study was conducted in the Barito watershed, more specifically in the province of South Kalimantan (Figure 1). In early 2021, this area was flooded, affecting about 5000 surrounding communities (Prihartini et al., 2021; Puspitarini, 2021). The flooding lasted for several days. The flood caused great economic and social losses (Priagung, 2021). Therefore, this site was selected as a study area to evaluate the distribution of flood events and the possible triggering factors. It is hoped that the results of this study can be taken into account in determining development management strategies for the study area. This research used radar and optical satellite imagery as input data. This radar image was used to map the distribution of flood inundation. The radar images used were mosaic images for July 2020 and mosaics for January 2021.

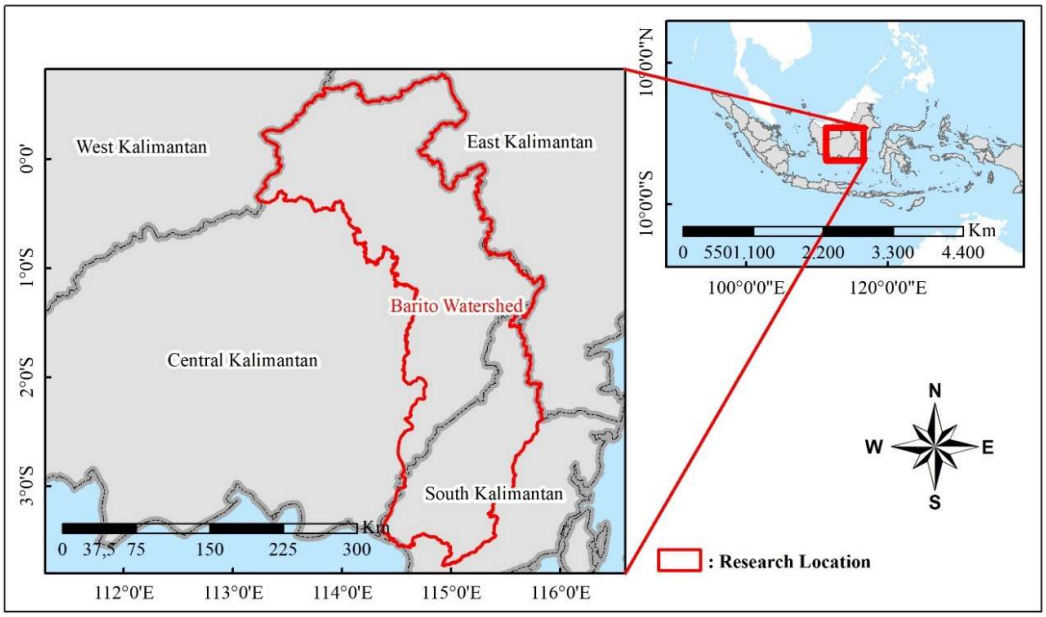

Figure 1. Research location in the Barito watershed.

Data availability

This study used VV polarization which is a type of polarization where the radar waves sent by the source and received by the sensor are vertically directed radar waves (DeVries et al., 2020). This polarization was chosen because most of the backscattering is more stable (Zhang et al., 2016). Polarization can separate water and non-water with better accuracy than VH polarization (Chulafak et al., 2021). In addition, the VV polarization was chosen, considering that Indonesia is a tropical region with quite a dense vegetation cover. Floods in vegetated locations are easier to detect using VV polarization (Zhang et al., 2020).

In addition to radar images, this study also used optical images of Landsat-8 Mosaic images in 2015 and Mosaic in 2020. These images were used to analyze changes in land cover use in the Barito watershed. The multi-temporal mosaic image in this study minimizes the influence of clouds in the research location. In this study, blue (B2), green (B3), red (B4), near-infrared (B5), short-wave infrared-1 (B6), and short-wave infrared-2 (B7) bands were used to determine the type of land use/land cover (LULC). Sentinel-1 and Landsat-8 images in this study can be accessed on the Google Earth Engine (GEE) platform.

The flood analysis

The flood analysis in this study consisted of three stages. First, performing flood inundation detection from Sentinel-1 imagery. The next was the evaluation of land use and cover changes from Landsat-8 imagery. Lastly, it overlayed the flood inundation detection results with the land use/cover in 2020.

Flood inundation detection

In this study, a threshold was used to determine flood inundation. Before calculating the threshold value, the first process was to prepare the input data. The input data used was the image of Sentinel-1 before and after the flood incident described in the previous section. A change detection process with a reduction operator was used to obtain the difference in image backscatter values before and after the flood event. The existence of a flood in the image after the surge is expected to provide a strong contrast. Meanwhile, the existing water bodies are expected not to change the backscatter value. The change detection data was inputted to get the flood inundation threshold value.

Usually, the threshold value is explicitly determined at a particular matter. However, each data at a different location or time is very dependent on the conditions at that location and time. That condition can make the threshold value applied to a specific place and time inappropriate if used for other sites and times. Therefore, the method of determining the threshold must be flexible and can adapt to data conditions. The Otsu method is a thresholding method whose value depends on the situation of the data because the matter is evaluated from the statistical significance of the data used. Thus, in this study, the Otsu method was used to detect flood inundation. The Otsu method in this study can be seen in equations 1 and 2 below (Chulafak et al., 2021):

$$\sigma_B^2(k) = \frac{\left[\sum_{i=1}^{L} i\frac{n_i}{N}\sum_{i=1}^{k}\frac{n_i}{N} - \sum_{i=1}^{k} i\frac{n_i}{N}\right]^2}{\sum_{i=1}^{k}\frac{n_i}{N}\left[1-\sum_{i=1}^{k}\frac{n_i}{N}\right]} \quad (1)$$

$$\sigma_B^2(k^*) = \max_{1\le k<L} \sigma_B^2(k) \quad (2)$$

where, σ_B^2 is inter-class variance, n_i is the number of pixels at location i, N is the total number of pixels, k is a list of potential thresholds, L is the grey levels, and k^* is the optimal threshold.

Mapping of land cover use change

Changes in land cover use were carried out using the change detection method. The post-classification comparison (PCC) approach was used to see changes in land cover use. The PCC method is one method that is often used in change detection (Tiede, 2014). A guided digital classification method was used to classify land cover use types from Landsat-8 satellite imagery. The classification algorithm used was the Random Forest algorithm with a prediction tree of one hundred. The Random Forest algorithm is a classifier that consists of a combination of prediction trees and depends on the value of each sample vector (Breiman, 2001). Random forest is one of the most efficient classification methods (Akar and Güngör, 2012). The random forest has several advantages over other classification methods. The benefits of Random Forest include having a faster sample calculation time, more stable parameters, and high accuracy (Pelletier et al., 2016). Random Forest Algorithm can be seen by using the following equation 3 (Breiman, 2001):

$$\{h(\boldsymbol{x}, \theta_k), k = 1, 2, \ldots.\} \quad (3)$$

where h is a random forest classification result, $\boldsymbol{x}$ is a sample, and θ_k It is a random unique vector class in random forest classification.

Mapping the distribution of flood inundation

The overlapping technique was used to determine the distribution of flood inundation locations. The overlapping process is a multi-criteria application of data layers (Faisal and Shaker, 2017). The results of flood inundation detection using the Otsu method overlapped with the land cover use classification in 2020. Thus, it can be seen that the distribution of flood inundation locations depends on land cover use.

Results

Flood inundation mapped

The Otsu method used in this study can detect flood inundation well. The detected flood inundation area can be seen in the blue polygon in Figure 2. Most of

the inundation occurred in the downstream region of the Barito Watershed. The flood inundation area detected using the Otsu method is 1,096.28 km^2.

Land used land cover change

Analysis of land cover change in the Barito watershed shows that there has been a change in land cover use in the Barito watershed from 2015 to 2020 (Figure 3). The results showed that during five years, there was a decrease in the area of primary forest by 13,000 ha, secondary forest by 116,000 ha, rice fields by 146,000 ha, and shrubs by 47,000 ha. On the other hand, there was a significant expansion of the plantation area of 219,000 ha.

Changes in land cover use in the Barito watershed presented in Table 1 show that in 2020 the Barito watershed is still dominated by primary forests with almost 70%. The secondary forest also has a fairly large proportion, around 11%. Thus the forest area in this watershed still dominates, with a total area of about 81% of the Barito watershed. In addition, the Barito watershed has been converted into a plantation area, which is 9% of the watershed in 2020.

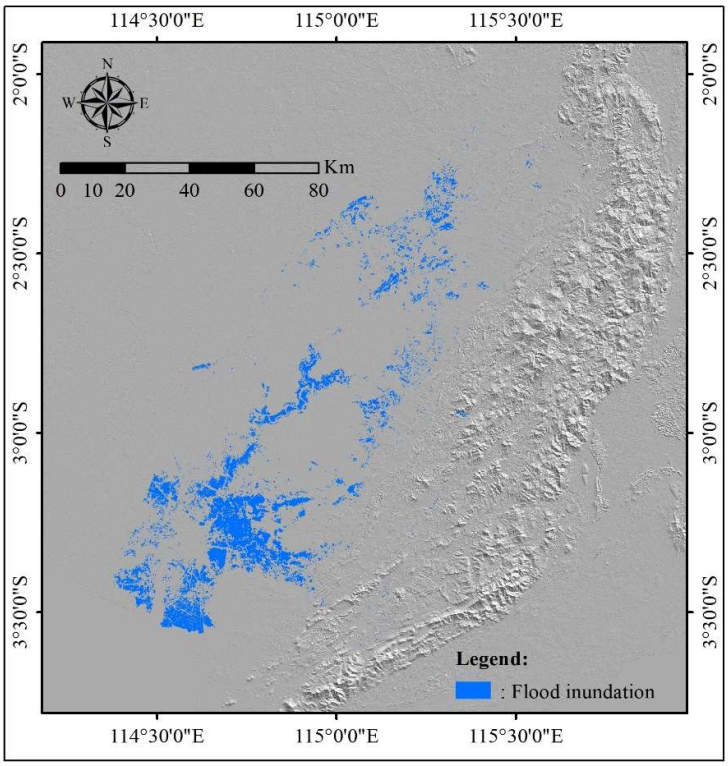

Figure 2. Flood inundation from Sentinel-1 imagery using the Otsu thresholding method.

Table 1. Calculation of the area of land use change in the Barito watershed.

No	LULC Class	LULC Area 2015		LULC Area 2020	
		Area (ha)	Area Proportion (%)	Area (ha)	Area Proportion (%)
1	Primary forest	4,612,208.19	69.19	4,599,188.04	68.99
2	Secondary forest	861,244.22	12.92	745,008.89	11.18
3	Dry farmland	379.50	0.01	119.85	0.00
4	Wet farmland	461,849.62	6.93	314,880.00	4.72
5	Settlement	70,722.80	1.06	85,602.21	1.28
6	Bare land	54,152.50	0.81	118,983.22	1.78
7	Plantation	433,456.51	6.50	652,372.52	9.79
8	Shrub	64,854.02	0.97	17,545.42	0.26
9	Fishpond	43,944.63	0.66	34,343.46	0.52
10	Water body	63,587.01	0.95	98,355.40	1.48

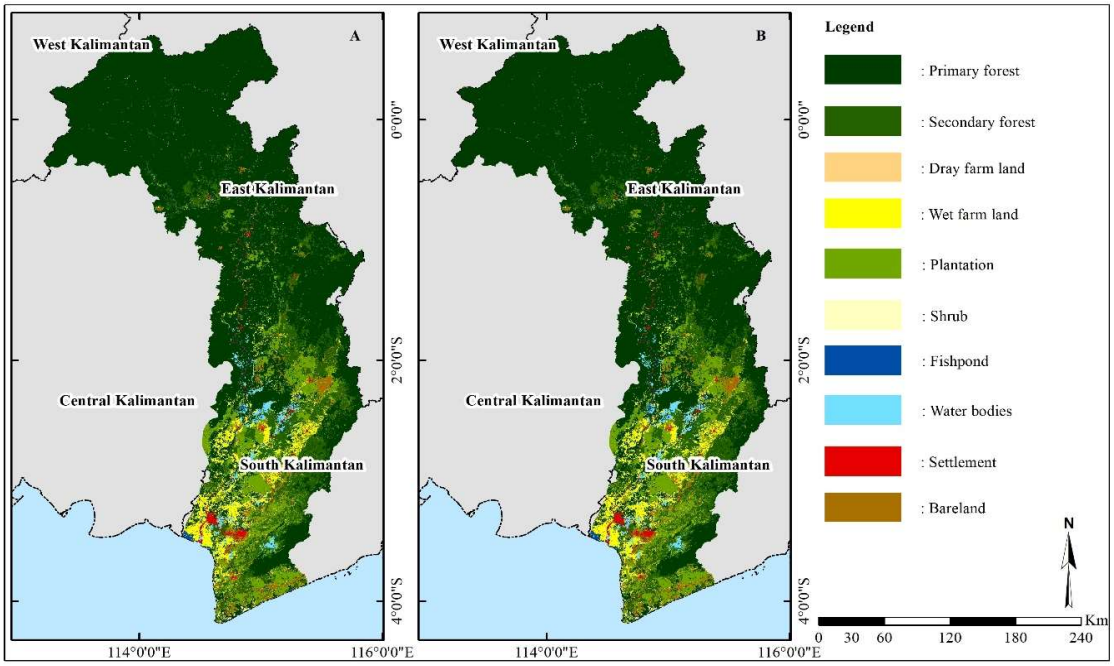

Figure 3. Land cover use from Landsat-8 imagery. (A) land cover use for the Barito watershed in 2015. (B) land cover use for the Barito watershed in 2020.

The distribution of flood inundation mapped

The overlapping flood inundation maps and land cover use produces a flood inundation distribution map. The highest proportion of flood inundation is in rice fields. Nearly 50% of the flood inundation is in the area. Floods that inundate rice fields have the potential to thwart harvests, thereby increasing the risk of food availability insecurity (Week and Wizor, 2020). It turns out that a reasonably large proportion also occurs in the type of land cover in the form of a body of water, which is 19%. Meanwhile, flood inundation in residential areas is only about 1%. The complete distribution of flood inundation is shown in Figure 4.

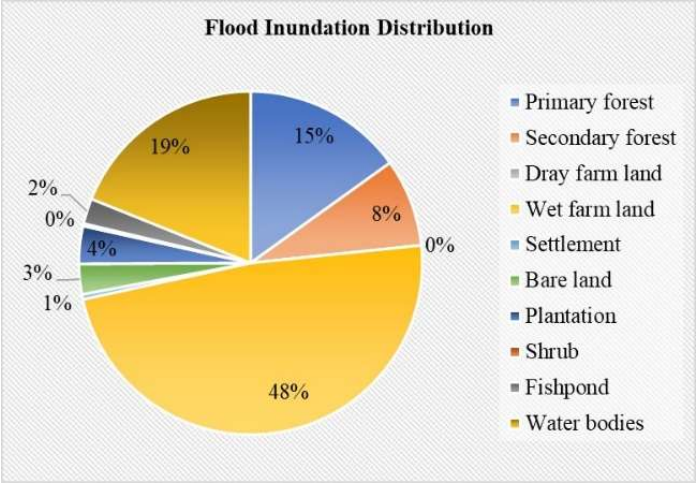

Figure 4. Distribution of flood inundation in the Barito watershed.

Discussion

The Otsu method used in this study produces a threshold of -2.74. Flood puddles are formed by pixels that have a value less than -2.74. The threshold value obtained differs from the value commonly used to separate water and land, which is 0 (reference). A threshold of 0 is usually used for a single image, where

the puddle is determined directly from the backscatter value received by the sensor. While in this study, data before and after the flood event were used that flood inundation is defined by the difference in backscatter values before and after the flood event.

From Figure 4, it can be seen that there are still flooded puddles detected in the area of the body of water. This phenomenon is due to flood waters that inundate areas of permanent water bodies. Flood water in which other particles are dissolved causes the backscatter to the Sentinel-1 sensor to be larger (Purinton and Bookhagen, 2020). The presence of dissolved particles in the water causes the surface texture to become rougher so that the water reflects more radar waves. Therefore, some areas of permanent water bodies have different negative backscatter values that are less than the threshold value. Judging from the distribution of flood inundation locations, most of them occur in wetland agricultural areas. These floods can potentially cause economic losses and can cause food availability insecurity (Week and Wizor, 2020). So it is necessary to know the factors that can encourage and cause this flood event so that plans can be determined so that similar events do not happen again.

LULC dynamics data is sufficient to illustrate that there has been a change in land use in the Barito Watershed area between 2015 and 2020. These changes can potentially affect the environmental response in capturing rainwater received by the Barito Watershed. Changes in land use cover, primarily the reduction in forest area, can potentially affect the hydrological process in this area (Anwar et al., 2011). Primary and secondary forests are vital in preventing rainwater from becoming surface runoff. The decrease in forest area can increase the discharge and surface runoff in the Barito Watershed (Salim et al., 2019). However, despite the changes, the forest coverage in this watershed is still extensive at around 81%. Therefore, further research is needed to ensure that changes in land cover use in the Barito Watershed are the main factors causing flooding in this area.

The increase in bare land and built-up land detected using the change detection method in this study needs attention. Population growth causes pressure on the environment due to increased housing and work needs, thus encouraging land function changes (Arfanuzzaman and Dahiya, 2019). There is a need for control and alternative solutions to minimize differences in the area. One of the efforts that can be proposed is the preparation and enforcement of regulations related to land use (Rosyidie, 2013). Engineering, such as providing a place to live vertically or in an environment-based deck, can be an alternative solution. The construction of flats can reduce the need for land. Thus, more land can be used as a catchment area.

The increase in the body of water can be caused by the area of shrubs in the form of swamps being submerged by water. Water covering the surface of the bush or grass makes the reflectance received by the sensor affected by the presence of water. An increase in the area of a water body can also be caused by the misclassification of a wet rice field area identified as a water body. These two phenomena cause the reflectance value received by the satellite image sensor to be a water reflectance so that the area is recognized as a body of water.

This study was limited to knowing the distribution of flood inundation locations. The method is sufficient to illustrate that there is a change in land cover use that can potentially be a factor causing flood events. Modeling by integrating other supporting data, such as altitude and rainfall data, can be further developed to determine the main factors causing flooding in this area. Floods can be generated and driven by factors, e.g., meteorology, ecology, population, water conservation, and government policies (Nie et al., 2012).

Research related to flooding, especially flood event modeling, has the potential to continue to be developed. Currently, modeling has been designed to predict LULC on the earth's surface based on remote sensing satellite imagery. It may be adopted to be applied in the research location to see how the land use/cover projection is at the research location. Thus, the research of determining the level of vulnerability to flooding can also be done, So that the government can determine a land use management plan based on that research.

Conclusion

This study shows that the use of change detection and Otsu threshold methods on multi-temporal sentinel-1 images can map the flood inundation area in the Barito watershed with an area of 109.628 ha. The combination of change detection and machine learning methods using the random forest algorithm on Sentinel-2 imagery detects changes in land use cover in the Barito Watershed from 2015 to 2020. The Barito Watershed has decreased the area of primary forest, secondary forest, fields, rice fields, bushes and ponds. Meanwhile, settlements, bare land, plantations, and water bodies have increased. Decreasing and increasing land use has affected flooding. This means that there is land degradation in the Barito watershed. The Otsu model can infer inundation from remote sensing data before and after a flood event.

Acknowledgements

The authors are grateful to the USGS, ESA, KLHK, BNPB, and GEE for providing free data for this research. This research was supported by PUTI NKB-617//UN2.RST/HKP.05.00/2020 from Universitas Indonesia. The authors are grateful to the National Disaster Management Agency for providing reference and sample data for flood disasters.

References

Acharya, T.D., Subedi, A., Yang, I.T. and Lee, D.H. 2017. Combining water indices for water and background threshold in Landsat image. P*roceedings* 2018(2):143, doi:10.3390/ecsa-4-04902.

Akar, Ö. and Güngör, O. 2012. Classification of multispectral images using random forest algorithm. *Journal of Geodesy and Geoinformation* 1(2):105-112, doi:10.9733/jgg.241212.1.

Amitrano, D., Di Martino, G., Iodice, A., Riccio, D. and Ruello, G. 2018. Unsupervised rapid flood mapping using Sentinel-1 GRD SAR images. *IEEE Transactions on Geoscience and Remote Sensing* 56(6):3290-3299, doi:10.1109/TGRS.2018.2797536.

Anurogo, W. 2017. Directional study on the conformity of the functions of the Progo watershed. *Media Trend* 12(2):98-107, doi:10.21107/mediatrend.v12i2.2721 (*in Indonesian*).

Anwar, M., Pawitan, H., Murtilaksono, K. and Jaya, I. 2011. Hydrologycal response due to deforestation in Barito Hulu Watershed, Central Kalimantan. *Jurnal Manajemen Hutan Tropika* 17(3):119-126 (*in Indonesian*).

Arfanuzzaman, M. and Dahiya, B. 2019. Sustainable urbanization in Southeast Asia and beyond: Challenges of population growth, land use change, and environmental health. *Growth and Change* 50(2):725-744, doi:10.1111/grow.12297.

Breiman, L. 2001. *Random Forest*. Machine Learning, 5-32.

Chulafak, G.A., Kushardono, D. and Yulianto, F. 2021. Utilization of multi-temporal Sentinel-1 satellite imagery for detecting aquatic vegetation change in Lake Rawapening, Central Java, Indonesia. *Applied Geography* 7(3):316-330, doi:10.1080/23754931.2021.1890193.

DeVries, B., Huang, C., Armston, J., Huang, W., Jones, J.W. and Lang, M.W. 2020. Rapid and robust monitoring of flood events using Sentinel-1 and Landsat data on the Google Earth Engine. *Remote Sensing of Environment* 240(October 2018), 111664, doi:10.1016/j.rse.2020.111664.

Echendu, A.J. 2020. The impact of flooding on Nigeria's sustainable development goals (SDGs). *Ecosystem Health and Sustainability* 6(1), doi:10.1080/20964129.2020.1791735.

Faisal, K. and Shaker, A. 2017. An investigation of GIS overlay and PCA techniques for urban environmental quality assessment: A case study in Toronto, Ontario, Canada. *Sustainability (Switzerland)* 9(3):1-25, doi:10.3390/su9030380.

Huang, M. and Jin, S. 2020. Rapid flood mapping and evaluation with a supervised classifier and change detection in Shouguang using Sentinel-1 SAR and Sentinel-2 optical data. *Remote Sensing* 12(13), doi:10.3390/rs12132073.

Lechner, A.M., Foody, G.M. and Boyd, D.S. 2020. Applications in remote sensing to forest ecology and management. *One Earth* 2(5):405-412, doi:10.1016/j.oneear.2020.05.001.

Li, J., Peng, B., Wei, Y. and Ye, H. 2021. Accurate extraction of surface water in complex environments based on Google Earth Engine and Sentinel-2. *PLoS ONE* 16(6):1-17, doi:10.1371/journal.pone.0253209.

Maria, R. and Lestiana, H. 2014. The effect of land use on groundwater conservation functions in the Cikapundung sub-watershed. *Jurnal RISET Geologi dan Pertambangan* 24(2):77-89, doi:10.14203/risetgeotam2014.v24.85 (*in Indonesian*).

Nguyen, H.T.T., Doan, T.M., Tomppo, E. and McRoberts, R.E. 2020. Land use/land cover mapping using multitemporal Sentinel-2 imagery and four classification. *Remote Sensing* 12(9):1367, doi:10.3390/rs12091367.

Nie, C., Li, H., Yang, L., Wu, S., Liu, Y. and Liao, Y. 2012. Spatial and temporal changes in flooding and the affecting factors in China. *Natural Hazards* 61(2):425-439, doi:10.1007/s11069-011-9926-1.

Nyamekye, C., Ghansah, B., Agyapong, E. and Kwofie, S. 2021. Mapping changes in artisanal and small-scale mining (ASM) landscape using machine and deep learning algorithms - a proxy evaluation of the 2017 ban on ASM in Ghana. *Environmental Challenges* 3(January), 100053, doi:10.1016/j.envc.2021.100053.

Özelkan, E. 2020. Water body detection analysis using NDWI indices derived from Landsat-8 OLI. *Polish Journal of Environmental Studies* 29(2):1759-1769, doi:10.15244/pjoes/110447.

Pelletier, C., Valero, S., Inglada, J., Champion, N. and Dedieu, G. 2016. Assessing the robustness of random forests to map land cover with high resolution satellite image time series over large areas. *Remote Sensing of Environment* 187:156-168, doi:10.1016/j.rse.2016.10.010.

Priagung, A. 2021**.** Analysis of environmental law violations that caused the January 2021 flood in Kalimantan. *Al Qisthas: Jurnal Hukum dan Politik Ketatanegaraan* 13(1):63-76, doi:10.37035/alqisthas.v13i1.4308 (*in Indonesian*).

Prihartini, P., Aini, M., Sya'diah, N. and Tazkianida, R.F. 2021. Social worker service model for flood disaster victims in Banjar City, South Kalimantan Province in 2021. *Jurnal Manajemen Bencana* 7(1):37-44, doi:10.33172/jmb.v7i1.694 (*in Indonesian*).

Purinton, B. and Bookhagen, B. 2020. Multiband (X, C, L) radar amplitude analysis for a mixed sand- and gravel-bed river in the eastern Central Andes. *Remote Sensing of Environment* 246(March):111799, doi:10.1016/j.rse.2020.111799.

Puspitarini, R.C. 2021. Perspective Seeing South Kalimantan Floods in 2021. *Jurnal Ilmu Sosial dan Politik* 1(1):1-10 (*in Indonesian*).

Ramakrishna, G., Solomon, R.G. and I. Daisy. 2014. Impact of floods on food security and livelihoods of Idp Tribal. *International Journal of Development and Economics Sustainability* 2(1):11-24.

Rosyidie, A. 2013. Floods: facts and impacts, as well as the effects of land use change. *Jurnal Perencanaan Wilayah dan Kota* 24(3):241-249, doi:10.5614/jpwk.2013.24.3.1 (*in Indonesian*).

Salim, A.G., Dharmawan, I.W.S. and Narendra, B.H. 2019. The effect of changes in forest land cover areas on the hydrological characteristics of the upper Citarum watershed. *Jurnal Ilmu Lingkungan* 17(2):333, doi:10.14710/jil.17.2.333-340 (*in Indonesian*).

Savitri, E. and Pramono, I. 2017. Flood analysis of upper Cimanuk 2016. *Jurnal Penelitian Pengelolaan Daerah Aliran Sungai* 1(2):97-110, doi:10.20886/jppdas.2017.1.2.97-110 (*in Indonesian*).

Shen, X., Anagnostou, E.N., Allen, G.H., Robert Brakenridge, G. and Kettner, A.J. 2019. Near-real-time non-obstructed flood inundation mapping using

synthetic aperture radar. *Remote Sensing of Environment* 221 (October 2018):302-315, doi:10.1016/j.rse.2018.11.008.

Solórzano, J.V., Mas, J.F., Gao, Y. and Gallardo-Cruz, J.A. 2021. Land use land cover classification with U-net: Advantages of combining Sentinel-1 and Sentinel-2 imagery. *Remote Sensing* 13(18), doi:10.3390/rs13183600.

Sugianto, S., Deli, A., Miswar, E., Rusdi, M. and Irham, M. 2022. The effect of land use and land cover changes on flood occurrence in Teunom Watershed, Aceh Jaya. *Land* 11(8):1271, doi:10.3390/land11081271.

Talukdar, S., Singha, P., Mahato, S., Shahfahad, Pal, S., Liou, Y.A. and Rahman, A. 2020. Land-use land-cover classification by machine learning classifiers for satellite observations-A review. *Remote Sensing* 12(7), doi:10.3390/rs12071135.

Tiede, D. 2014. A new geospatial overlay method for the analysis and visualization of spatial change patterns using object-oriented data modeling concepts. *Cartography and Geographic Information Science* 41(3):227-234, doi:10.1080/15230406.2014.901900.

Traore, M., Takodjou Wambo, J.D., Ndepete, C.P., Tekin, S., Pour, A.B. and Muslim, A.M. 2020. Lithological and alteration mineral mapping for alluvial gold exploration in the southeast of Birao area, Central African Republic using Landsat-8 Operational Land Imager (OLI) data. *Journal of African Earth Sciences* 170(February):103933, doi:10.1016/ j.jafrearsci.2020.103933.

Uddin, K., Matin, M.A. and Meyer, F.J. 2019. Operational flood mapping using multi-temporal Sentinel-1 SAR images: A case study from Bangladesh. *Remote Sensing* 11(13), doi:10.3390/rs11131581.

Wahyuni, W., Arsyad, U., Bachtiar, B.and Irfan, M. 2017. Identification of water catchment areas in the upper Malino watershed sub-watershed Jeneberang river basin, Gowa Regency. *Jurnal Hutan dan Masyarakat* 9(2):93-104, doi:10.24259/jhm.v9i2.2891 (*in Indonesian*).

Week, D.A. and Wizor, C.H. 2020. Effects of flood on food security, livelihood and socio-economic characteristics in the flood-prone areas of the core Niger Delta, Nigeria. *Asian Journal of Geographical Research* 3(1):1-17, doi:10.9734/ajgr/2020/v3i130096.

Yulianto, F., Kushardono, D., Budhiman, S., Nugroho, G., Chulafak, G.A., Dewi, E.K. and Pambudi, A.I. 2022. Evaluation of the threshold for an improved surface water extraction index using optical remote sensing data. *Scientific World Journal* 2022, doi:10.1155/2022/4894929.

Yulianto, F., Nugroho, G., Aruba Chulafak, G. and Suwarsono, S. 2021. Improvement in the accuracy of the post classification of land use and land cover using Landsat 8 data based on the majority of segment-based filtering approach. *Scientific World Journal* 2021, doi:10.1155/2021/6658818.

Zhang, M., Chen, F., Liang, D., Tian, B. and Yang, A. 2020. Use of Sentinel-1 GRD SAR images to delineate flood extent in Pakistan. *Sustainability (Switzerland)* 12(14):1-19, doi:10.3390/su12145784.

Zhang, M., Li, Z., Tian, B., Zhou, J. and Tang, P. 2016. The backscattering characteristics of wetland vegetation and water-level changes detection using multi-mode SAR: A case study. *International Journal of Applied Earth Observation and Geoinformation* 45:1-13, doi:10.1016/j.jag.2015.10.001.